metals

MDPI

Review

Application of Ultrasonic-Enhanced Leaching for the Recovery of Metal Elements from Mineral Raw Materials and Secondary Resources

Yusufujiang Mubula [1,2], Mingming Yu [1,2,*], Heyue Niu [1,2], Zhehan Zhu [1,2] and Kun Xu [1,2]

[1] Jiangxi Provincial Key Laboratory of Low-Carbon Processing and Utilization of Strategic Metal Mineral Resources, Ganzhou 341000, China; 6720221227@mail.jxust.edu.cn (Y.M.); 6720230100@mail.jxust.edu.cn (H.N.); 6120240303@mail.jxust.edu.cn (Z.Z.); 6120240289@mail.jxust.edu.cn (K.X.)

[2] School of Resources and Environmental Engineering, Jiangxi University of Science and Technology, Ganzhou 341000, China

* Correspondence: ymm1990@jxust.edu.cn

Abstract

Driven by the practical needs of reducing mining costs and protecting the environment, and with the growing focus on the green and efficient recovery of metal elements (Cu, Mn, Ni, Co, Li, V, Al, Fe, REEs) from mineral raw materials and secondary resources, ultrasonic-enhanced leaching has emerged as an effective method for achieving the resource recovery of the aforementioned metals. As the ultrasonic-enhanced leaching process can effectively recover metal elements from mineral resources and secondary resources, it can effectively reduce the energy consumption, shorten the recycling time, and effectively improve the efficiency of the recovery of metal elements in the recycling process. This paper provides a comprehensive overview of the latest references and scientific knowledge in the field of ultrasonic-enhanced leaching, classifies and summarizes the application of ultrasonic-enhanced leaching in the recovery of metal elements from mineral resources and secondary resources, and discusses the mechanisms of ultrasonic-enhanced leaching in detail.

Keywords: ultrasonic enhanced leaching; hydrometallurgy; metal elements; secondary resources

Academic Editor: Man Seung Lee

Received: 4 September 2025
Revised: 5 October 2025
Accepted: 6 October 2025
Published: 8 October 2025

Citation: Mubula, Y.; Yu, M.; Niu, H.; Zhu, Z.; Xu, K. Application of Ultrasonic-Enhanced Leaching for the Recovery of Metal Elements from Mineral Raw Materials and Secondary Resources. *Metals* **2025**, *15*, 1115. https://doi.org/10.3390/met15101115

1. Introduction

With the increasing demand for non-renewable metal elements [1], the massive consumption of lithium, cobalt, vanadium, rare earths, and other metal resources by modern electronic products and industries has caused precious metal elements to face the dilemma of resource depletion [2,3]. This has led to the efficient utilization of non-renewable mineral resources, the recovery of precious metal elements from secondary resources, and the reuse of precious metal elements becoming more and more urgent [4,5]. Currently, the most mainstream methods for recovering metal elements are hydrometallurgical methods and pyrometallurgical methods [6–9]. However, these traditional processes (hydrometallurgical and pyrometallurgical) generally suffer from problems such as a low leaching efficiency, long leaching time, high reagent usage, and high energy consumption [10–20]. So, there is a pressing need to explore an efficient and environmentally friendly method to recover metal elements from minerals and secondary resources [21–26]. To improve the recovery efficiency of metal elements, researchers have compensated for the shortcomings of the traditional method by introducing assisted technologies [27,28]. In recent years, the application of ultrasound in leaching processes has become more and more widespread, which is

due to the cavitation, mechanical, and thermal effects of ultrasound that make it possible to improve the leaching efficiency and shorten the leaching time in the recovery process [29].

The application of ultrasound in the recovery of metal elements mainly utilizes the cavitation effect of ultrasound. The impact of cavitation on the reaction system primarily manifests in both physical and chemical effects. Specifically, its physical effects involve the transformation of gas nuclei already dissolved in the solution, such as O_2, N_2, and other gases, into microbubbles through the alternating acoustic pressure. These microbubbles then undergo oscillation and growth, ultimately leading to their rupture, as illustrated in Figure 1A [30]. When microbubbles expand rapidly and collide with each other during transfer in solution, the gas or vapor inside the bubbles is compressed, and the collapse of the cavitation bubbles in a very short time generates a huge amount of energy locally (1018 kW/m^3) [31]. Meanwhile, the periodic generation and collapse of cavitation bubbles produces shock waves/microjets with pressure amplitudes of about 240 MPa and molecular motion velocities of up to 1700 m/s. These strong shock waves/microjets will cause the local temperature near the bubble to rise sharply to 2000~10,000 K. The huge energy released from the bubbles during transient cavitation will have a strong impact and stripping effect on the insoluble impurities on the surface of the object, causing the impurities to fall out of the solution. In addition, transient cavitation also has a dissolving effect on the surface components of the object, which can expose its internal components [32], as shown in Figure 1B. The sharp increase in temperature inside the bubble causes the decomposition of water vapor and oxygen to form various oxidants, such as ·OH, H_2O_2, oxygen atoms, and O_3 [33], as shown in Figure 1C. The above various oxidants produced in solution have a strong oxidative decomposition effect, which has a good promotion effect on the leaching of metal elements in mineral resources and secondary resources [34]; the above processes are the main reasons for most of the physical and chemical effects of ultrasound in solid/liquid or liquid/liquid systems [35–37].

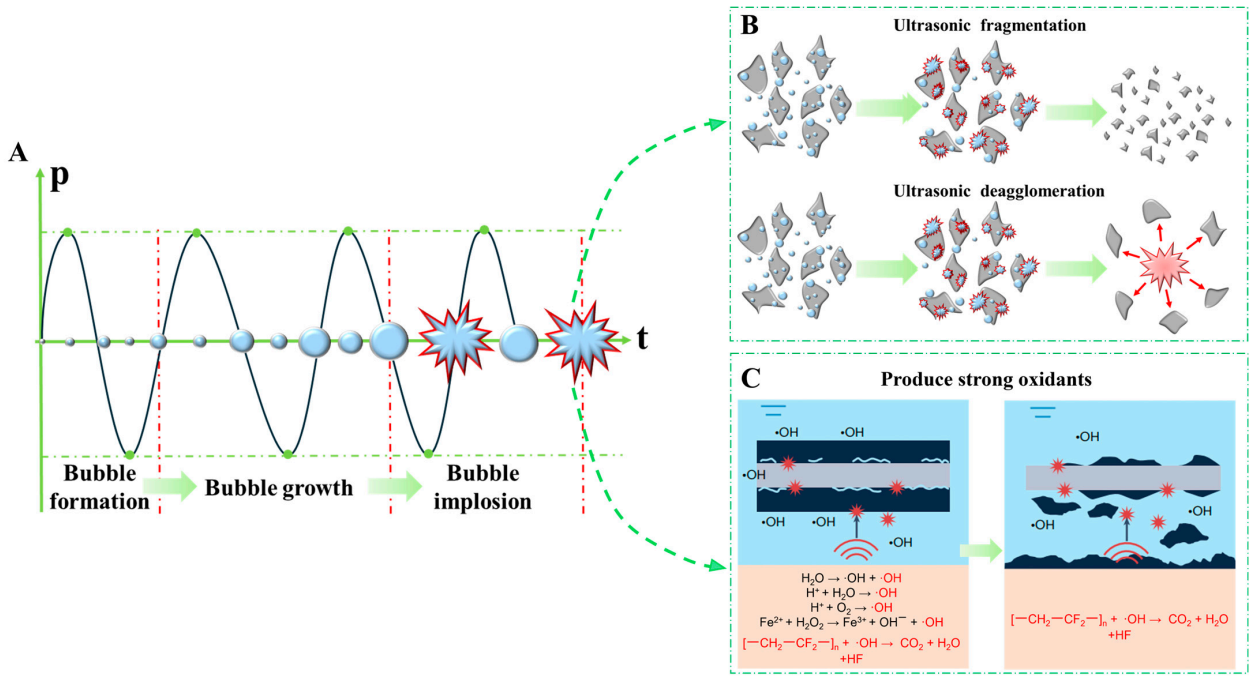

Figure 1. (**A**) Steps in cavitation activity along time: bubble formation, growth, and implosion; (**B**) effect of ultrasonic cavitation on particle size; (**C**) ultrasonically activating the oxidizing agents can produce strong oxidants. This image is reprinted from [36–38], with permission from Elsevier, 2022, 2021, 2022.

Since the cavitation of ultrasound has the above physical and chemical effects, the use of this effect to recover metal elements from mineral resources and secondary resources has become a research hotspot. This paper summarizes and compares the existing representative studies on the recovery of metal elements using ultrasound.

According to the existing research, ultrasonic-enhanced leaching is different from conventional leaching [30,32]. The ultrasonic-enhanced leaching method is widely used in the recovery of metal elements from minerals and secondary resources [22,35,39,40]. The existing representative studies are classified into two major categories: the recovery of valuable metal elements from minerals and that from secondary resources. These two categories are further subdivided into four subsections based on the recovery of common metal elements and rare metal elements, as shown in Figure 2. The research on the ultrasonic-assisted enhanced leaching of valuable elements is also summarized and compared in terms of experimental equipment, research methodologies, experimental conditions, and mechanism analyses.

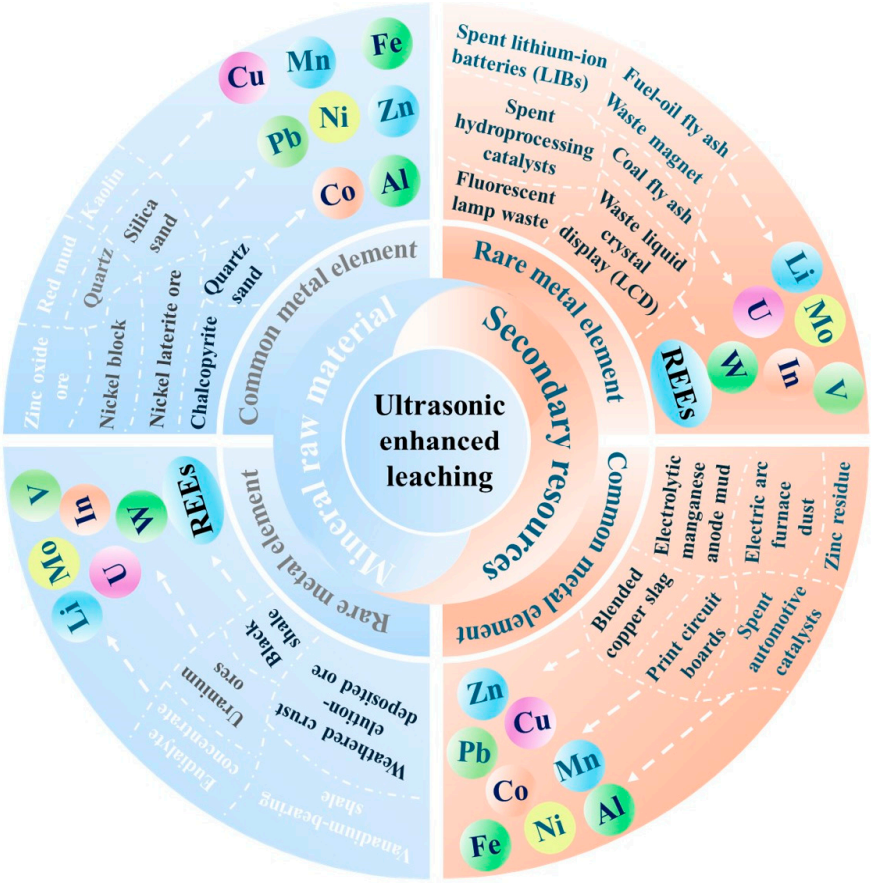

Figure 2. Ultrasonic-enhanced leaching in the recovery of metallic elements from minerals and secondary sources.

2. Recovery of Metal Elements from Mineral Raw Material

2.1. Recovery of Common Metal Elements

In recent years, the study of the enhanced leaching of metal elements by ultrasonic assistance has obtained better results, and the ultrasonic synergistic strengthening process was analyzed to confirm that it was effective in improving the leaching efficiency of metal elements. Xue et al. [41] investigated the oxidative leaching process of nickel (Ni) directly from nickel sulfide ores with oxidizing agents under the action of ultrasound. The results show that an 82.95% leaching rate for Ni can be achieved through ultrasonic-enhanced leaching. Li et al. [42] studied a method for recovering nickel (Ni) from nickel

ores with the assistance of ultrasound. The results showed that the ultrasonic cavitation effect could strip off the oxide film on the nickel surface, which increased the reaction area, promoted the liquid–solid reaction, accelerated the yield of nickel sulfate, effectively shortened the reaction time (by 50%), and improved the reaction efficiency (by 50%). The maximum leaching rate of this process is limited. Under the optimal process conditions (30% sulfuric acid concentration, 10% hydrogen peroxide, temperature of 333 K, ultrasonic power of 200 W, and reaction time of 4 h), the nickel leaching rate is only 60.41%, and the conventional leaching rate is even lower (43.87%), which is far from achieving an efficient recovery of nickel resources. For high-purity nickel blocks (with a nickel mass fraction of 99.96%), nearly 40% of the nickel remains unleached, leading to a low resource utilization and failing to meet the core requirement of a "high recovery rate" in industrial production.

The use of ultrasonic-enhanced leaching technology in the recovery of zinc (Zn) from zinc ore has achieved good results. He et al. [43] proposed a novel synergistic system combining mechanical and ultrasonic activation for Zn leaching from ZnO ores. The results showed that the median particle size of ZnO ore could be crushed from ~29.2 μm to ~178 nm, as shown in Figure 3A. The microscopic morphology of the original and activated ZnO is shown in Figure 3B,C. This is accompanied by the small-size crushing of particles, the creation of new surfaces, point defects, and dislocations in the crystal structure, and polycrystalline transformations ready to disrupt the crystal structure and gradually transform it into a disordered state [44,45]. Furthermore, the XRD spectra of raw ZnO and activated ZnO in Figure 3D show that the ZnO raw ore consists of ZnO, $ZnFe_2O_4$, and $Zn_6Al_2O_9$ with good crystallinity. The modeling results in Figure 3E show that the combination of ultrasonic and mechanical activation effectively reduces the activation energy (Ea) (from 54.6 kJ/mol to 26.4 kJ/mol), whereas ultrasonic and mechanical activation can only reduce the activation energy to 44.9 kJ/mol and 41.5 kJ/mol, respectively. The dual action of ultrasonic waves has been strengthened, which results in an increase in the recovery of Zn (about 12%). The research content only analyzes the influence of ultrasonic power (50 W–150 W) on extraction, and does not involve variable experiments on ultrasonic frequency (fixed at 20 kHz in the paper) and ultrasonic operation modes (such as continuous ultrasound and intermittent ultrasound). Different ultrasonic frequencies will change the intensity and distribution of the cavitation effect, and intermittent ultrasound may affect energy accumulation and slurry stability. The lack of these parameters makes it impossible to fully reveal the synergistic mechanism between ultrasound and bead milling.

The recovery of copper (Cu) from copper-bearing ores can be carried out through ultrasonic-enhanced leaching. Wang et al. [46] investigated the reaction kinetics of Cu leaching from chalcopyrite in an acidic ferric sulfate medium with and without ultrasound assistance. Compared with conventional leaching methods, the ultrasound-assisted leaching process not only has a high leaching rate and short leaching time, but also has a low reagent dosage and high selectivity.

By summarizing the studies on the recovery of metals from minerals using ultrasonication-enhanced leaching, it can be concluded that ultrasonication-enhanced leaching is obviously superior to the traditional leaching methods. In addition, ultrasonication leaching can be combined with other leaching techniques to further improve the strengthening effect of ultrasonication leaching. We list representative research data in Table 1 on the recovery of common metal elements from minerals using ultrasonication-enhanced leaching.

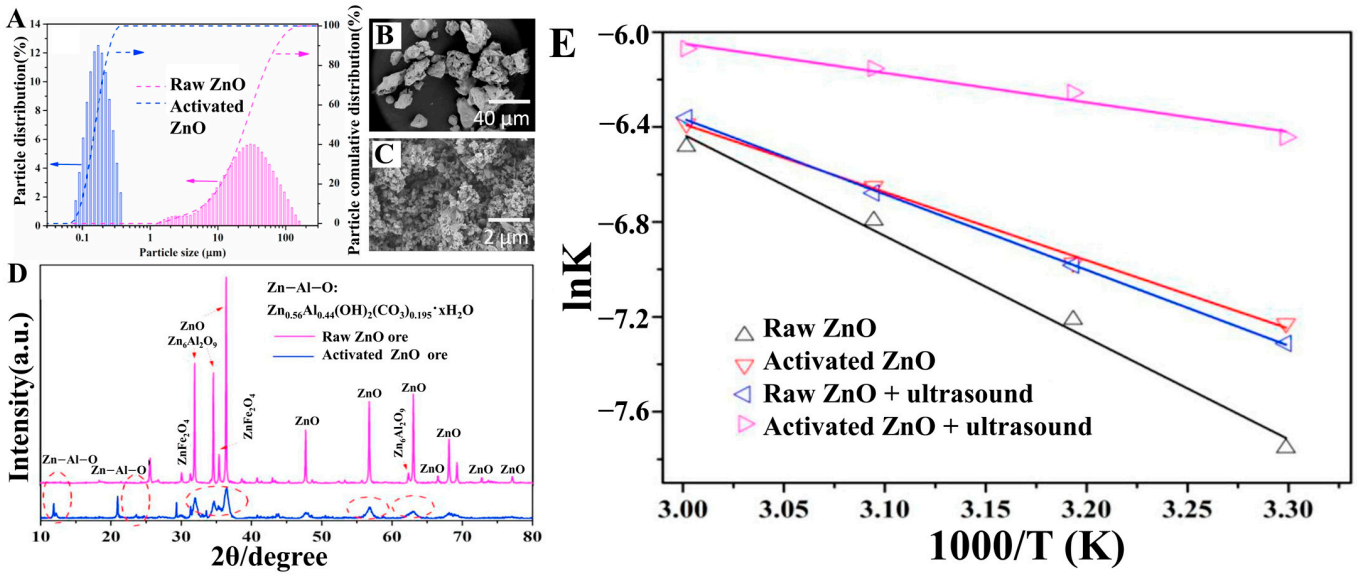

Figure 3. (**A**) Particle size distributions of raw and mechanically activated ZnO ores; (**B**) SEM images of raw ZnO ore; (**C**) mechanically activated ZnO ore; (**D**) XRD patterns of raw and mechanically activated ZnO ores; (**E**) Arrhenius plots for the leaching kinetics of raw and activated ZnO ores leaching in the presence of ultrasound. The combination figure is an integration of the figures, reprinted from [43], with permission from Elsevier, 2018.

Table 1. Recovery of common metal elements from minerals.

Target Elements	Raw Materials	Chemical Reagents	Temperature	Time	Ultrasonic Power/Frequency	Leaching Rate	Ref.
Ni	Nickel sulfide ore	$Na_2S_2O_8$-$AgNO_3$	70 °C	120 min	220 W	82.95%	[41]
	Nickel block	H_2SO_4-H_2O_2	60 °C	240 min	200 W	60.41%	[42]
	Nickel laterite ore	H_2SO_4	95 °C	10 min	720 W	96.18%	[29]
Zn	Zinc oxide ore	NH_3–$(NH_4)_2SO_4$	30 °C	60 min	600 W	83.33%	[47]
	Zinc oxide ore	NH_3-$C_6H_5O_7(NH_4)_3$	25 °C	120 min	600 W	88.57%	[48]
	Zinc oxide ore	H_2SO_4	60 °C	90 min	150 W	75%	[43]
Cu	Chalcopyrite	$Fe_2(SO_4)_3$-H_2SO_4	80 °C	300 min	80 W	57.5%	[46]
	Deep-sea manganese nodules	$(NH_4)_2S_2O_3$	85 °C	90 min	100 W	93%	[49]
Al	Quartz	Na_2CO_3	80 °C	25 min	150 W	42.3%	[50]
Fe	Quartz sand	H_3PO_4	80 °C	240 min	150 W	77.1%	[51]
	Silica sand	$H_2C_2O_4$	95 °C	30 min	150 W	75.4%	[52]

2.2. Recovery of Rare Metal Elements

The recovery of vanadium (V) from low-grade vanadium ores using ultrasonic-enhanced leaching has also become a research hotspot. Chen et al. [53] systematically investigated the effects and mechanisms of ultrasound and CaF_2 on V leaching from vanadium-bearing shales. The synergistic effect in this study enhances vanadium extraction through the mechanism of "structure destruction—mass transfer acceleration—chemical activation", with specific manifestations as follows: the activation energy of the leaching reaction is further reduced to 27.61 kJ/mol under the synergistic effect, which is much lower than the 82.50 kJ/mol of ultrasound alone and 50.70 kJ/mol of CaF_2 alone, significantly lowering the reaction energy barrier and making vanadium dissolution easier to occur; the mineral structure is destroyed more thoroughly—the cracks generated by ultrasonic cavitation provide deeper diffusion channels for HF, while HF specifically breaks down the mica lattice, and their combined action makes the diffraction peaks of

mica almost disappear (the attenuation of mica characteristic peaks in the residue of the "ultrasound + 3 wt% CaF_2" group is the most significant), resulting in the highest degree of vanadium release; there is a dual improvement in mass transfer and reaction efficiency—ultrasound promotes the adsorption and diffusion of H^+, F^{--}, and HF on the mineral surface, while CaF_2 continuously generates HF to maintain a high-activity leaching environment; the combination of the two maximizes both the concentration of effective leaching agents in the pulp and the contact efficiency between these agents and the active sites of minerals, ultimately increasing the vanadium leaching rate by 66.28%, which is higher than the 26.97% improvement by ultrasound alone and 60.35% improvement by CaF_2 alone. The synergistic enhancement process is illustrated in Figure 4.

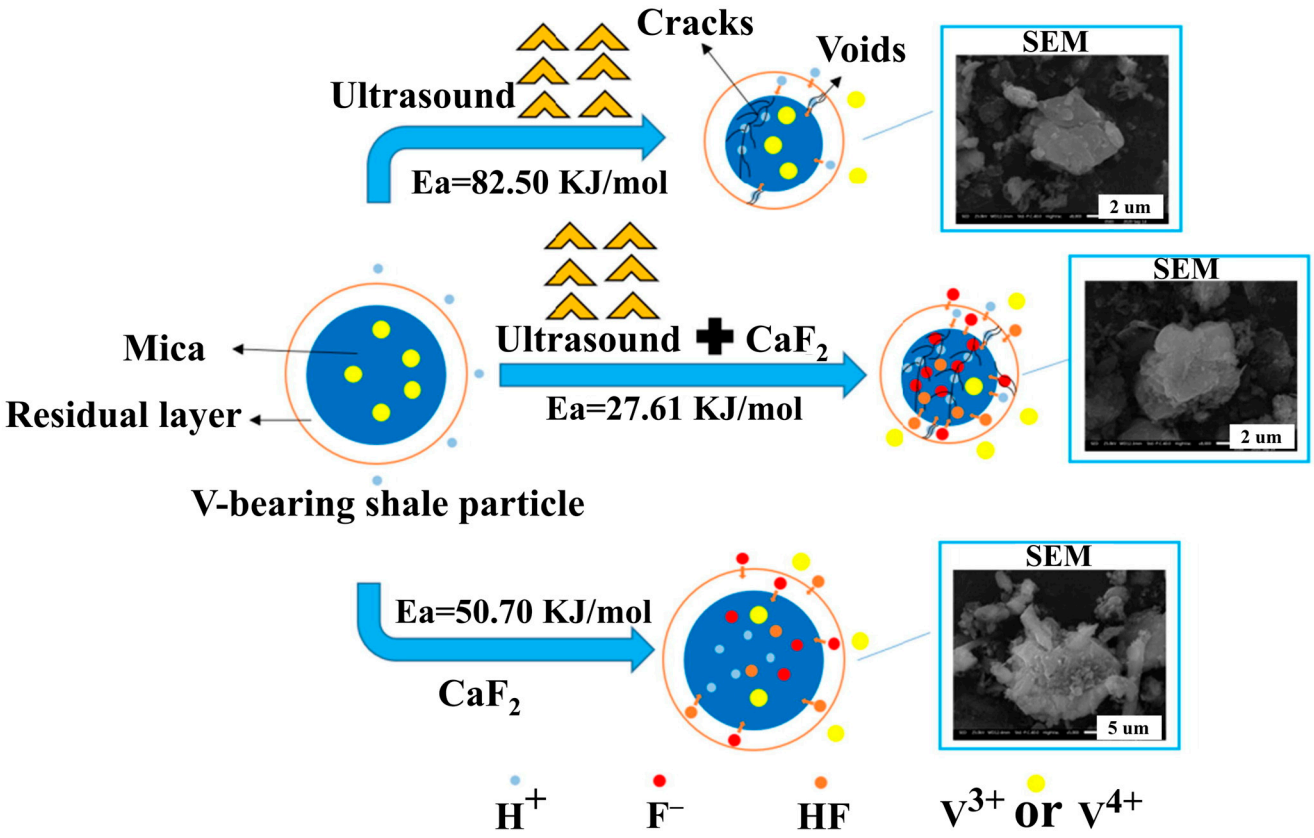

Figure 4. Synergetic mechanism for vanadium leaching out of V-bearing shale improved by ultrasound and CaF_2. This image is reprinted from [53], with permission from Elsevier, 2016.

Tungsten (W) has been widely used in the chemical industry, machinery and equipment manufacturing, and other fields [54]. In recent years, the recovery of W from tungsten ore using ultrasonic-enhanced leaching technology has achieved better results. Örjan et al. [55] investigated the effects of ultrasonic cavitation on W leaching efficiency. It was shown that the leaching efficiency of W using ultrasonic cavitation energy supplemented by 130 kWh/kg was 71.5%, while the leaching rate without ultrasound was 36.7%. The results confirmed that ultrasonic cavitation can effectively reduce energy consumption and improve W recovery. The introduction of ultrasonic waves can effectively promote the collision chance between the leaching agent and mineral particles, thus promoting the efficient dissolution and leaching of W from tungsten ore.

The use of ultrasonic-enhanced leaching for the recovery of rare precious metals has also been increasingly studied [56]. In recent years, the use of ultrasound-assisted leaching techniques has effectively improved the leaching efficiency of Au from gold ores and gold concentrates. Gui et al. [57] investigated the oxidation of sulfide coatings on Au

surfaces using ozone and ultrasonic synergistic pretreatment and studied the mechanism of synergistic-enhanced oxidation. After 4 h of ozone and ultrasonic pretreatment, the leaching rate of Au increased from 49.12% to 93.52%. Ultrasound and ozone pretreatment not only oxidized the pyrite encrustation, but also effectively destroyed the pyrite encrustation and inhibited the secondary encrustation in a short time, as shown in Figure 5A–C. At the same time, ultrasonic treatment significantly reduces the particle size of difficult-to-select gold ores, increases their specific surface area, shown in Figure 5D,E, intensifies the oxidation process during pretreatment (ultrasound and ozone), and can significantly increase the leaching efficiency of Au. The process flow mentioned that ozone has an extremely low solubility in aqueous solutions (only 14 mmol/L at 20 °C). Even when introduced into the system via aeration, a large amount of ozone is discharged with the exhaust gas without participating in the reaction. This not only causes a waste of oxidant but also requires an additional investment in exhaust gas treatment equipment (such as the "ozone tail gas treatment device" mentioned in the paper), increasing the complexity and energy consumption of the process. Meanwhile, to achieve the desired oxidation effect, a relatively high ozone flow rate (3.44 g/h as the optimal value) must be maintained, which further raises the cost of ozone generation and reduces the economic viability of the process.

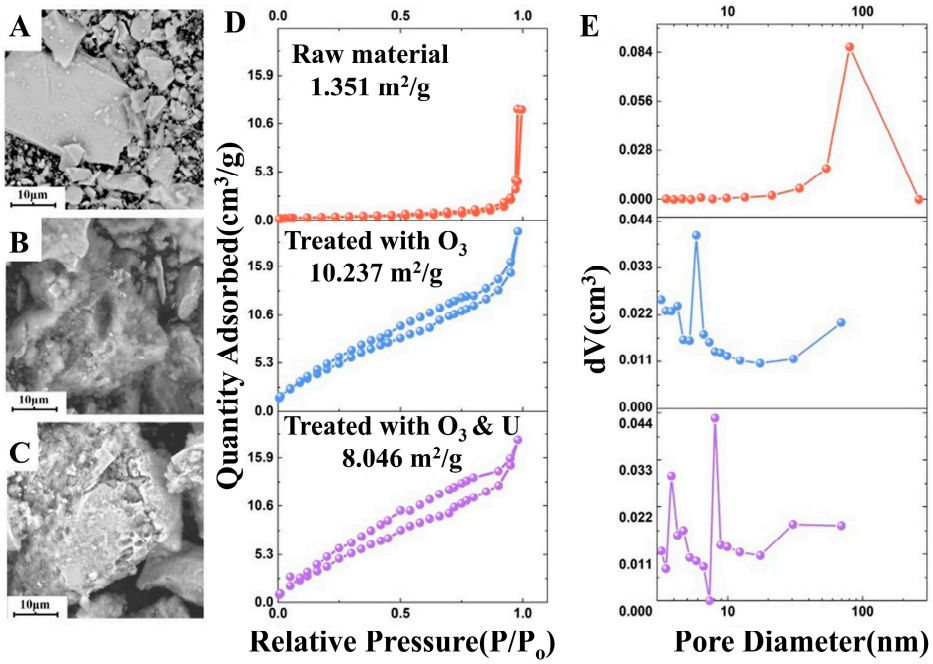

Figure 5. SEM images of (**A**) raw material, (**B**) ore treated with O_3, and (**C**) ore treated with ozone and ultrasound, and their BET images (**D**,**E**). The combination figure is an integration of the figures, reprinted with permission from [57], with permission from Elsevier, 2022.

Larrabure et al. [19] investigated the ultrasound-assisted leaching of Ag-containing polymetallic (Mn-Fe-Pb) sulfides. It was shown that ultrasound-assisted leaching decreases surface Mn by dissolving oxidizing substances, exposing the surface of fresh sulfides and increasing Ag leaching. Ultrasound-assisted leaching could obtain a higher Ag leaching of 60%, while conventional leaching could only extract 25%. Cilek et al. [58] investigated the application of ultrasound in the cyanidation reaction of refractory silver ores. Ultrasonic waves can effectively improve the leaching rate of Ag (the 24 h leaching rate of sono-cyanidation is approximately 15.5% higher than the 48 h leaching rate of conventional cyanidation, achieving a 50% reduction in cyanidation time), and the use of ultrasonic waves can greatly reduce the cyanidation time without affecting the leaching efficiency of Ag, being 13% more efficient with ultrasound than without ultrasound. Experiments

showed that the effect of ultrasonic frequency (37 kHz and 80 kHz) on silver recovery is negligible (p-value = 0.907 in the analysis of variance). Changing the frequency alone cannot improve the leaching efficiency; instead, it increases the complexity of equipment selection. In industrial settings, it is necessary to match ultrasonic transducers with specific frequencies. The meaningless frequency variable will lead to an increase in equipment costs, and it is impossible to optimize the leaching process for ores with different characteristics (such as the content of silver sulfide minerals) by adjusting the frequency.

By summarizing the relevant studies on the recovery of rare metals from minerals using ultrasonication-enhanced leaching, we can determine that ultrasonic-enhanced leaching is a highly efficient recovery method, which points to a new direction for the future exploration of assisted enhanced leaching technology. We list the representative research data of the recovery of rare metal elements from minerals using ultrasonication-enhanced leaching methods in Table 2.

Table 2. Recovery of rare metal elements from minerals.

Target Elements	Raw Materials	Chemical Reagents	Temperature	Time	Ultrasonic Power/Frequency	Leaching Rate	Ref.
V	Vanadium-bearing shale	H_2SO_4-CaF_2	95 °C	30 min	900 W	92.93%	[40]
W	Scheelite	Na_3CO_3	90 °C	450 min	1000 W	22.5%	[54]
	Scheelite	HNO_3	80 °C	360 min	131 kWh/kg	71.5%	[55]
	Scheelite	NaOH	90 °C	146 min	176 W	90%	[59]
Au	Refractory gold ores	NaClO-NaOH	30 °C	120 min	200 W	68.55%	[56]
	Refractory gold ores	HCl-Cl_2	50 °C	120 min	300 W	50%	[60]
	Refractory gold ore	$Na_3(CN)_3C_3H_3N_6O_3$	80 °C	240 min	480 W	93.52%	[57]
Ag	Refractory gold ore	$Na_3(CN)_3C_3H_3N_6O_3$	80 °C	240 min	480 W	61.25%	[57]
	Refractory silver ores	NaCN	30 °C	2880 min	100 W	90%	[58]
REEs	Weathered crust elution-deposited ore	$MgSO_4$	25 °C	30 min	700 W	99%	[61]
	Eudialyte concentrate	HNO_3	80 °C	140 min	22 KHz	94.5%	[62]

3. Recovery of Metal Elements from Secondary Sources

3.1. Recovery of Common Metal Elements

With the significant popularization of electronic and technological products, the consequent generation of secondary resources containing valence metal elements is increasing. In recent years, many researchers have confirmed the superiority of assisted enhanced recovery methods over conventional recovery methods [63]. Esmaeili et al. [64] investigated ultrasound-assisted bio acid leaching for the leaching of metals from spent lithium-ion batteries. Organic acids from lemon juice and H_2O_2 were used as leaching agents. The results showed that metal recovery dropped sharply without $H_{22}O_{22}$ and lemon juice, decreased much less without ultrasound, and reached 100% for Li and Co when ultrasonic treatment was applied for 35 min of leaching. Xiao et al. [65] investigated an ultrasound-assisted leaching method for the leaching of metals from spent lithium-ion batteries. The entire leaching process shortened more than 50% of the leaching time due to the localized thermal effect of ultrasonics. The use of ultrasound to improve the mass transport of metal ions in the residue layer of used lithium-ion batteries during organic acid leaching at low temperatures (50 °C) can facilitate the recovery of battery metals.

Ding et al. [66] investigated the effect of ultrasound on the leaching of gallium (Ga) and Zn from corundum flue dust and its mechanism. The leaching efficiencies of Ga and Zn were increased from 62.78% and 82.56% to 94.43% and 99.57%, respectively, under the effect of ultrasonic-enhanced leaching. By comparing the SEM images of conventional leaching,

shown in Figure 6A–C, and ultrasonic leaching, shown in Figure 6D,E, it was found that the enhancement of the leaching rate and leaching efficiency by ultrasound was mainly because ultrasonic action breaks the particle agglomerates into small pieces or cracks, which enhances the diffusion of sulfuric acid and the product layer on the surfaces of particles. Through the experimental phenomena and leaching kinetic modeling, the mechanistic processes of conventional and ultrasonic-enhanced leaching, shown in Figure 6G, were deduced, and the superiority of ultrasonic-enhanced leaching over conventional leaching was confirmed by comparison. Corundum flue dust contains a large amount of silicates and aluminosilicates. Concentrated sulfuric acid preferentially reacts with these silicates and aluminosilicates to form by-products such as aluminum sulfate and silicon sulfate, resulting in the consumption of part of the sulfuric acid before it participates in the leaching of gallium (Ga) and zinc (Zn). Experiments show that, when the sulfuric acid concentration exceeds 25 wt%, there is no significant increase in the leaching rates of Ga and Zn, which confirms the existence of an ineffective consumption of sulfuric acid. This further increases the reagent cost and the subsequent wastewater treatment load.

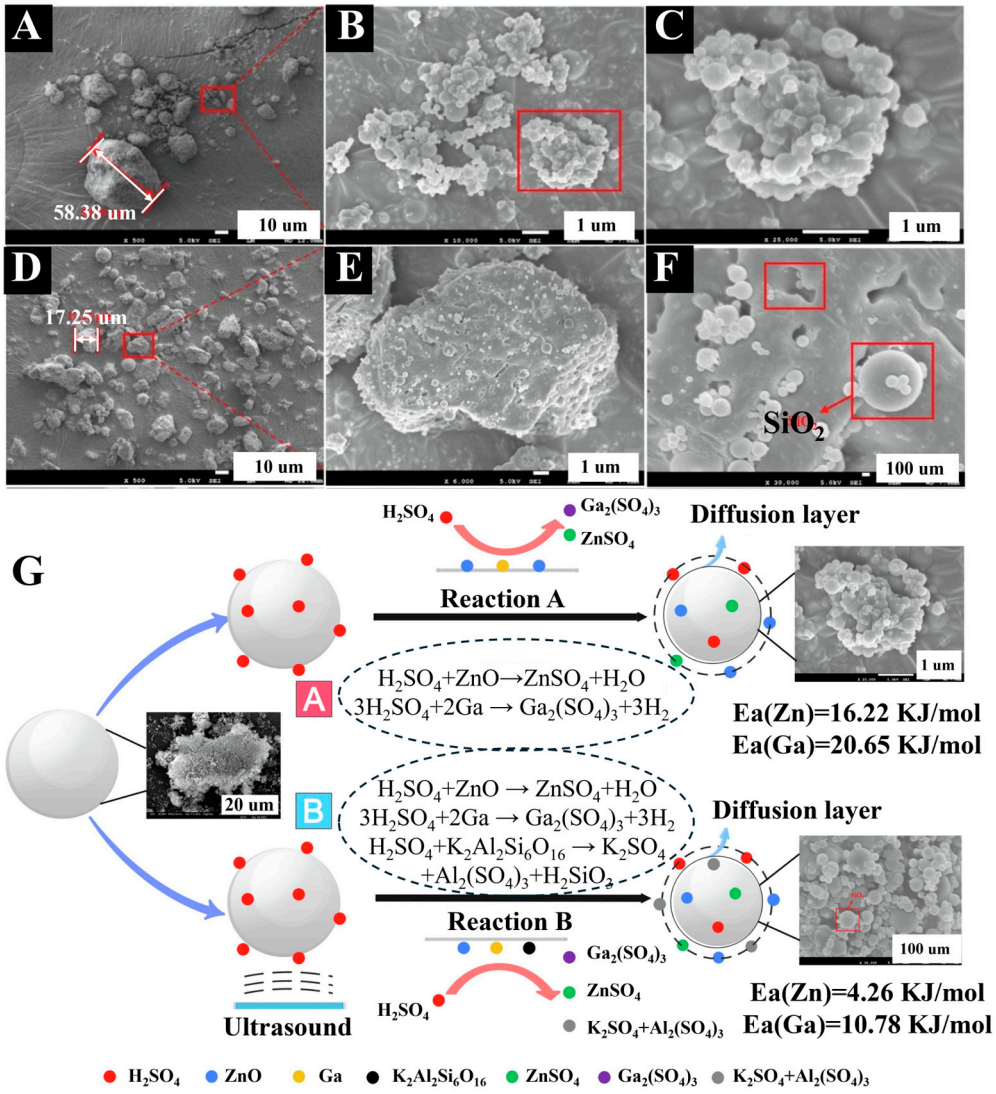

Figure 6. (**A**–**C**) SEM image of conventional leaching residue; (**D**–**F**) SEM image of ultrasonic leaching residue; (**G**) the mechanism of ultrasound assisted leaching. The combination figure is an integration of the figures, reprinted from [66], with permission from Elsevier, 2022.

Xin et al. [39] enhanced the leaching process of germanium-containing slag powder by using the innovative method of combining ultrasound and oxygen, and the equipment

is shown in Figure 7A. The use of ultrasound combined with oxygen can obtain a stronger oxidizing capacity and achieve a higher leaching efficiency of Zn and germanium (Ge), by 4.92% and 9.80%, respectively, than that in conventional leaching. By comparing the SEM images of the raw ore, shown in Figure 7B,C, and the leaching slag, shown in Figure 7D,E, with ultrasound combined with oxygen, it was found that using ultrasound combined with oxygen could not only destroy the crystal structure of the minerals and reduce the crystallinity of the minerals, but also break the minerals, open the mineral inclusions, leach out the sulfide, release the encapsulated germanium, and ultimately increase the leaching efficiency of Zn and Ge. Through the experimental phenomena and the leaching kinetic model, the mechanism process of conventional leaching and ultrasonic-enhanced leaching, shown in Figure 7F, was inferred. This is a green, efficient, and environmentally friendly waste recycling method. Experiments were conducted using a small-volume 500 mL reactor, where ultrasonic energy could be uniformly distributed. However, when scaled up to an industrial cubic-meter-scale reactor, the ultrasonic energy attenuates significantly with propagation distance (over 60% energy loss at 1 m from the transducer). This leads to the excessive fragmentation of raw material particles in areas close to the transducer (generating fine powders that clog the filter screen), while insufficient cavitation effects occur in areas far from the transducer (ZnS inclusions remain unbroken, preventing germanium exposure). Consequently, the overall leaching efficiency may decrease by 10–15%. Although this issue can be mitigated by using a multi-transducer array, it will further increase equipment investment and energy consumption.

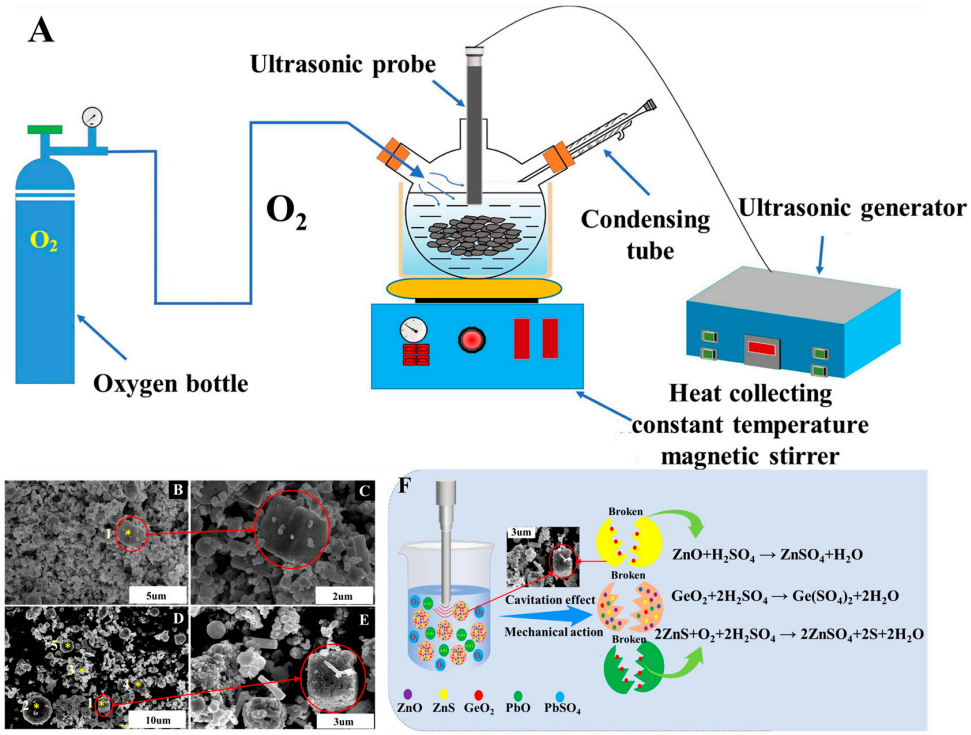

Figure 7. (**A**) Schematic diagram of the experimental setup for ultrasonic- combined with oxygen-enhanced leaching; (**B**,**C**) SEM-EDS image of germanium-containing slag dust, * represents the microstructure of germanium-containing slag dust; (**D**,**E**) SEM-EDS image of ultrasound combined with oxygen residue, * represents the microstructure of the reaction residue from ultrasound combined with oxygen; (**F**) schematic diagram of ultrasound combined with oxygen leaching mechanism analysis. The combination figure is an integration of the figures, reprinted from [39], with permission from Elsevier, 2022.

Ultrasonic-enhanced leaching has also made good progress in the recovery of precious metals. Hosseinzadeh et al. [67] used the ultrasound-assisted Fenton-like leaching of

precious metals from spent automotive catalysts. The recovery efficiencies of Al and Ce with ultrasound were 12.2% and 33.8% higher than without ultrasound for the same reaction time. Zhu et al. [68] investigated the process of acid-free in situ chemical oxidation ultrasound-enhanced persulfate leaching of Ag from zinc slag. The study finds that the Ag leaching efficiency reached 91.09%. Ultrasonication lowered the reaction barrier and improved the silver leaching efficiency. As ultrasound reduced the activation energy from 112.47 kJ/mol to 65.23 kJ/mol and shortened the leaching time and improved the leaching efficiency (the experiments were conducted within a unified temperature range of 323 K–353 K (50–80 °C), which covers the temperature intervals used in both the single-factor experiments and kinetic analysis), the leaching mechanism of the Ag element was deduced by analyzing the reaction process, shown in Figure 8. The experiments showed that the leaching rates of associated metals (In: 75.11%, Zn: 51.74%, Ge: 43.12%) in zinc leaching residue by this process are much lower than that of silver (91.09%), and no subsequent separation and recovery scheme is mentioned. In industry, besides silver, associated metals such as In and Ge in zinc leaching residue are high-value scattered metals. The low leaching rates lead to resource waste, and the industrial chain advantage of the "synergistic recovery of multiple metals" is not formed, which reduces the overall economic viability of the process.

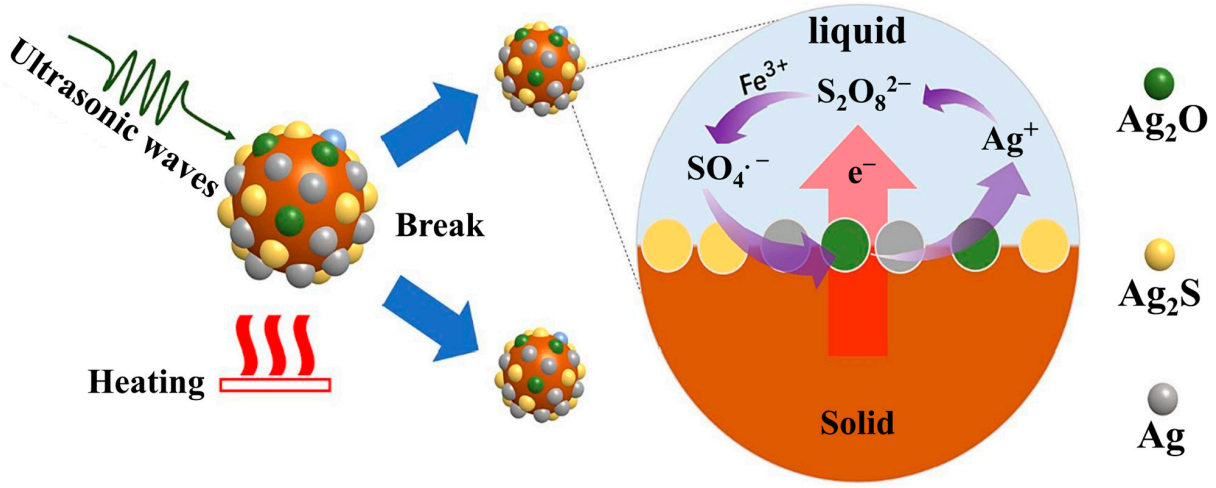

Figure 8. Reaction mechanism diagram. This image is reprinted with permission from [68], with permission from Elsevier, 2024.

Ultrasonic-enhanced leaching has achieved better research results in recovering Fe and Pb and in removing Fe from waste materials. Kong et al. [69] investigated the ultrasound-assisted leaching process for Fe removal from silica powder waste slag and optimized the leaching conditions to achieve an Fe removal rate of 95.24%. By introducing ultrasound-assisted leaching, the leaching time can be effectively shortened, and the removal efficiency can be improved. Xie et al. [70] investigated the microwave-coupled ultrasonic method for extracting Pb from electrolytic manganese anode sludge, and determined the flow of assisted recovery methods through experiments and modeling analysis, as shown in Figure 9. The results showed that microwave roasting promoted the conversion of MnO_2 to Mn_2O_3 and Mn_3O_4, which greatly facilitated the subsequent leaching process of Pb, and the introduction of ultrasonic waves made it possible to rapidly strip the mineral particles attached to the surface of inclusions, fillers, and impurities, exposing more active surfaces to participate in the leaching reaction and facilitating the contact between the leaching agent, cleaning agent, and particles, effectively enhancing the leaching process, realizing a leaching efficiency of Pb up to 86.98%. During the roasting process, $Pb_{22}Mn_{88}O_{1166}$ in the raw material decomposes to form PbO_{22}, and part of the PbO_{22} may further decompose into

PbO, which volatilizes with the flue gas (TG analysis shows that PbO_{22} starts to deoxygenate at 403.6 °C). Although the experiment is equipped with an exhaust gas treatment device (ammonia water + dilute NaOH + activated carbon), it does not detect the lead content in the exhaust gas. If the exhaust gas treatment is incomplete during industrial scaling-up, it will cause lead vapor pollution, requiring an additional investment in high-efficiency dust removal (such as electrostatic precipitation) and adsorption equipment.

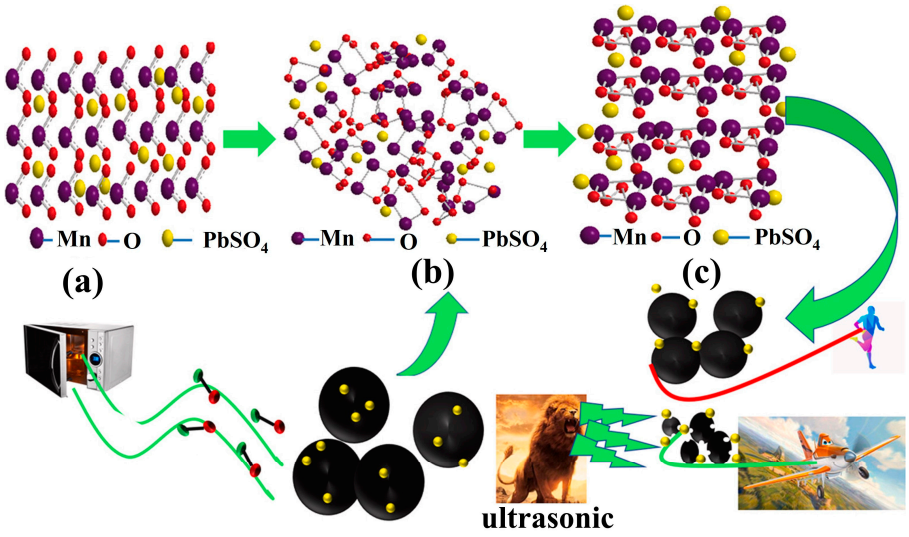

Figure 9. (**a**–**c**) The schematic diagram of ultrasonic-enhanced leaching. This image is reprinted from [70], with permission from Springer, 2021.

By summarizing the relevant studies on the recovery of common metal elements from secondary resources using ultrasonication-enhanced leaching, it can be concluded that ultrasonication-enhanced leaching is obviously superior to the traditional leaching method, and the recovery of metal elements can be efficiently achieved by ultrasonication-enhanced leaching, and the reaction time and the amount of chemicals can be shortened by ultrasonication-enhanced leaching. Ultrasonic-enhanced leaching is an efficient and green recovery method. For readers to read more intuitively and quickly, we list representative research data in Table 3 on the recovery of common metal elements from secondary resources using ultrasonication-enhanced leaching.

Table 3. Recovery of common metal elements from secondary sources.

Target Elements	Raw Materials	Chemical Reagents	Temperature	Time	Ultrasonic Power/Frequency	Leaching Rate	Ref.
Ni	Spent catalysts	HNO_3	90 °C	50 min	30 KHz	95%	[71]
	Spent lithium-ion batteries (LIBs)	lemon juice–H_2O_2	40 °C	35 min	37 KHz	100%	[64]
	Spent LIBs	citric or acetic	50 °C	1440 min	110 W	99%	[65]
Zn	Electric arc furnace dust	H_2SO_4	80 °C	30 min	60 W	90%	[8]
	Corundum flue dust	H_2SO_4	90 °C	50 min	900 W	99.57%	[66]
	Zinc residue	H_2SO_4	65 °C	180 min	160 W	80%	[72]
Cu	Copper anode slime	H_2SO_4-$Na_2S_2O_8$	50 °C	50 min	400 W	98.11%	[73]
	Print circuit boards	spent etching solution	25 °C	30 min	300 W	93.76%	[74]
	Copper anode slime	Ultrasound Lixiviant: H_2SO_4	Room temperature	600 min	800 W	85.18%	[75]
	Blended copper slag	Lixiviant: H_2O_2-CH_3COOH	65 °C	60 min	10% ultrasound power	93%	[76]
Al	Spent automotive catalysts	$FeSO_4$-H_2O_2	70 °C	40 min	37 KHz	81.7%	[67]
	Aluminum dross	NaOH	50 °C	240 min	100 W	60%	[77]
Fe	Silicon diamond wire saw cutting waste	H_2SO_4	60 °C	50 min	270 W	95.24%	[69]
	Boron carbide waste- scrap	H_2SO_4	50 °C	50 min	210 W	94.5%	[78]

3.2. Recovery of Rare Metal Elements

Ultrasonic-enhanced leaching technology has achieved good results in the recovery of rare metals from secondary resources. Ghasemi et al. [79] used ultrasonic and hydrogen peroxide-assisted sulphuric acid leaching to extract V and yttrium (Y) from fly ash. Their study finds the recoveries of V and Y were 100% and 97%, respectively. Enhanced leaching by ultrasound allowed the leaching agent to degrade and diffuse into the coal ash particles for an efficient recovery of metal elements. Shruti et al. [80] utilized the synergistic action of Escherichia coli and ultrasound for the bioleaching of spent catalysts containing Mo, Ni, and Al. The use of a discontinuous ultrasonic treatment increased the molybdenum leaching efficiency from 46% to 54%. It was confirmed that the metal leaching efficiency of multiple ultrasonic treatments was higher than that of one continuous ultrasonic treatment. This study lacks comprehensive control groups, including "ultrasonic leaching without bacteria", "bacterial leaching without ultrasound", and "chemical leaching + ultrasound". As a result, it is impossible to clearly distinguish the independent contribution ratios of ultrasound's role in promoting bacterial growth, its mechanical damage effect on the catalyst structure, and the synergistic effect of these two roles in metal leaching. In addition, no control groups with different initial pH values (e.g., 7.0, 8.0, 9.0) or temperatures (e.g., 30 °C, 37 °C, 40 °C) were set up, making it difficult to rule out the interactive influence between environmental factors and ultrasound. Improvements are needed in subsequent research.

The recovery of the "industrial vitamins" of rare earth elements from secondary sources by ultrasonically enhanced leaching has been studied with good results, and the recycling of rare earth elements has been realized. Maryam et al. [81] used an ultrasonically enhanced leaching process to recover lanthanum (La) from fluid cracking catalysts. The high efficiency of ultrasonic-enhanced leaching achieved a recovery of 97.1% of rare earth elements, which is simpler and faster than the existing methods and minimizes energy and reagent consumption, while reducing costs and environmental benefits. Behera et al. [82] investigated the application of ultrasound- and microwave-assisted techniques for the dissolution of neodymium (Nd) from spent magnets using organic reagents. Under ultrasound-assisted leaching conditions, the almost total dissolution of Nd (~99.99%) was achieved by ultrasonic-enhanced leaching, with a reduction of 120 min in the leaching time compared to conventional mechanically agitated leaching (240 min for 65.03% of Nd). From the SEM results of the scrap magnet samples before and after the ultrasonic/microwave treatment, the enhancement of Nd leaching is mainly due to the cavitation effect of ultrasonic waves and the high thermal energy generated by microwaves to destroy the solid matrix of the scrap magnets, shown in Figure 10, resulting in the diffusion of Nd metal ions into the leaching phase.

In this study, only the shrinking core model and shrinking sphere model were used to fit the kinetic data, while the change in activation energy (E_a) was not calculated. This makes it impossible to quantify the enhancement degree of ultrasound/microwave on the leaching process from an energy perspective. Furthermore, the kinetic parameters of the two energy fields (ultrasound and microwave) acting alone and in combination were not compared, so the potential synergistic mechanism between them cannot be revealed.

By summarizing the related studies on the recovery of rare metal elements from secondary resources using ultrasonic-enhanced leaching, it can be concluded that the recovery of Li, V, Co, Mo, and REEs can be efficiently achieved using ultrasonic-enhanced leaching, and the reaction time and the amount of chemicals can be lessened by ultrasonic-enhanced leaching. We list representative research data in Table 4 on the recovery of rare metal elements from secondary resources using ultrasonication-enhanced leaching.

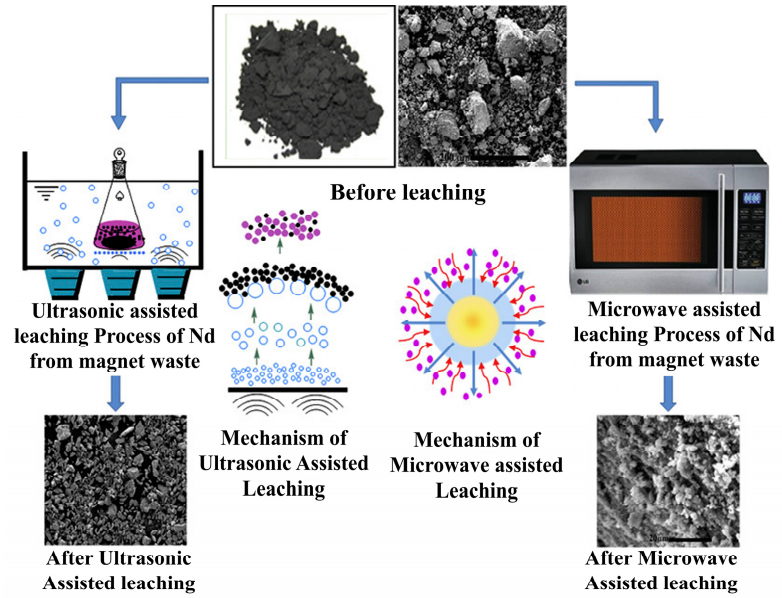

Figure 10. Ultrasonic/microwave process mechanism. This image is reprinted from [82], with permission from Springer, 2019.

Table 4. Recovery of rare metal elements from secondary resources.

Target Elements	Raw Materials	Chemical Reagents	Temperature	Time	Ultrasonic Power/Frequency	Leaching Rate	Ref.
Li	Spent LIBs	H_2SO_4-H_2O_2	30 °C	30 min	360 W	98.62%	[83]
	Spent LIBs	DL-malic acid-H_2O_2	80 °C	30 min	90 W	98%	[84]
V	Chromium-vanadium slag	H_2SO_4	60 °C	60 min	800 W	90.89%	[85]
	Coal fly ash	H_2SO_4-H_2O_2	50 °C	60 min	60 KHz	100%	[79]
Mo	Spent hydroprocessing catalysts	Critic acid	60 °C	360 min	320 W	95%	[86]
	Spent hydrodesulphurization catalysts	NaOH	80 °C	10 min	200 W	66%	[87]
	Spent hydrodesulphurization catalysts	Na_2CO_3	55 °C	120 min	600 W	94.3%	[88]
REEs	Spent fluid cracking catalysts	HCl	60 °C	60 min	200 W	97.1%	[81]
	LCD screen wastes	$P_2O_7^{4-}$	30 °C	60 min	120 W	85%	[89]
	Fluorescent lamp waste	HNO_3	20 °C	1440 min	120 W	95%	[90]
	Waste magnet	CH_3COOH	30 °C	120 min	90 W	99.99%	[82]

4. Conclusions

In this review, we systematically summarize the latest research results representative of ultrasonic-enhanced leaching technology (under an atmospheric pressure), classify and summarize them according to the types of recovered raw materials and elements, and describe the latest advances in the use of ultrasound enhancement for the recovery of various metals from ores and secondary resources and their corresponding enhancement mechanisms. Based on the literature review, we reach the following conclusions and outlook:

(1) By comparing the ultrasonic-enhanced leaching method with the traditional leaching method, the physicochemical properties and reaction mechanisms of ultrasonic-enhanced leaching are summarized, and three advantages of ultrasonic-enhanced leaching are summarized: (i) The use of the ultrasonic cavitation physical effect on the raw material particles of the crushing changes the morphology of the particles (reduces the size of the particles, destroys the surface morphology to increase the specific surface area, and removes the surface of the raw material of the passivation

layer), which is conducive to the mass transfer and diffusion of chemical agents on the particle surface and in the solution and the increase in the collision frequency between the leaching agent molecules and the raw material. (ii) The ultrasonic-enhanced leaching method can effectively reduce the activation energy of the leaching reaction, accelerate the leaching reaction efficiency, and realize the efficient leaching and recovery of metal elements. (iii) By using the chemical effect of ultrasonic cavitation to generate a strong oxidizing reagent (·OH or H_2O_2), the strong oxidizing reagent generated by the ultrasound replaces the chemical reagent, which improves the leaching efficiency and reduces the consumption of chemical reagents, realizing the cost savings and efficiency improvement of the leaching reaction process.

(2) The combined use of ultrasonic-enhanced leaching with new green enhanced methods (applied electric field, microwave heating) and reagents (microorganisms, organic acids, ionic liquids) can be adopted for the efficient recycling of low-grade minerals and secondary resources. The huge potential in the recovery of metal elements through ultrasound, in combination with active agents or other processes, requires further research. In addition, numerical simulations can be performed using software such as ANSYS Fluent (ANSYS Fluent, 2025 R2, ANSYS Inc., Canonsburg, PA, USA) [91] and MATLAB (MATLAB, R2025a, The MathWorks, Inc., Natick, MA, USA) [92], which can optimize the experimental parameters and reveal the strengthening mechanism [93]. The traditional method of high energy consumption and serious secondary pollution is transformed into a green and sustainable recycling method. However, based on the ultrasonic-enhanced leaching process, most of the research is in the laboratory stage; the small processing sample size, the limited ultrasonic cavitation area, and the poor stability of long-time operation are the main constraints for the industrial application of ultrasonic-enhanced leaching technology. In order to further promote the industrial application of ultrasonic leaching, systematic research should be conducted according to the types of samples to be treated and the ultrasonic leaching parameters to achieve better results.

Author Contributions: Y.M.: conceptualization, methodology, software, validation, formal analysis, investigation, writing—original draft preparation, writing—review and editing, visualization. M.Y.: conceptualization, resources, supervision, project administration, funding acquisition. H.N.: investigation, data curation, visualization. Z.Z.: methodology, validation, formal analysis, data curation, writing—original draft preparation. K.X.: methodology, validation, formal analysis, writing—review and editing. All authors have read and agreed to the published version of the manuscript.

Funding: This research was funded by the National Natural Science Foundation of China (52464025), Natural Science Foundation of Jiangxi Province (20224BAB204038), Young Elite Scientists Sponsorship Program by CAST (2022QNRC001), Academic and Technical Leaders Project of Major Disciplines in Jiangxi Province (20243BCE51072), Ganzhou Science and Technology Innovation Talent Project (2023CYZ26999), and Jiangxi Provincial Key Laboratory of Low-Carbon Processing and Utilization of Strategic Metal Mineral Resources (2023SSY01041). The APC was funded by National Natural Science Foundation of China (52464025).

Data Availability Statement: No new data were created or analyzed in this study. Data sharing is not applicable to this article.

Acknowledgments: Thanks to the National Natural Science Foundation of China (NSFC) and the Natural Science Foundation of Jiangxi Province.

Conflicts of Interest: The authors declare the following financial interests/personal relationships which may be considered as potential competing interests: Yu Mingming reports financial support was provided by the Natural Science Foundation of the Jiangxi Province. Yu Mingming reports financial support was provided by the Young Elite Scientists Sponsorship Program by CAST. The

remaining authors declare that the research was conducted in the absence of any commercial or financial relationships that could be construed as a potential conflict of interest.

References

1. Makuza, B.; Tian, Q.; Guo, X.; Chattopadhyay, K.; Yu, D. Pyrometallurgical options for recycling spent lithium-ion batteries: A comprehensive review. *J. Power Sources* **2021**, *491*, 229622. [CrossRef]
2. Anderson, A.; Rezaie, B. Geothermal technology: Trends and potential role in a sustainable future. *Appl. Energy* **2019**, *248*, 18–34. [CrossRef]
3. Amigues, J.-P.; Le Kama, A.A.; Moreaux, M. Equilibrium transitions from non-renewable energy to renewable energy under capacity constraints. *J. Econ. Dyn. Control* **2015**, *55*, 89–112. [CrossRef]
4. Jurasz, J.; Canales, F.A.; Kies, A.; Guezgouz, M.; Beluco, A. A review on the complementarity of renewable energy sources: Concept, metrics, application and future research directions. *Sol. Energy* **2020**, *195*, 703–724. [CrossRef]
5. Qazi, A.; Hussain, F.; Rahim, N.A.; Hardaker, G.; Alghazzawi, D.; Shaban, K.; Haruna, K. Towards Sustainable Energy: A Systematic Review of Renewable Energy Sources, Technologies, and Public Opinions. *IEEE Access* **2019**, *7*, 63837–63851. [CrossRef]
6. Bao, S.; Tang, Y.; Zhang, Y.; Liang, L. Recovery and Separation of Metal Ions from Aqueous Solutions by Solvent-Impregnated Resins. *Chem. Eng. Technol.* **2016**, *39*, 1377–1392. [CrossRef]
7. Abkhoshk, E.; Jorjani, E.; Al-Harahsheh, M.; Rashchi, F.; Naazeri, M. Review of the hydrometallurgical processing of non-sulfide zinc ores. *Hydrometallurgy* **2014**, *149*, 153–167. [CrossRef]
8. Brunelli, K.; Dabalà, M. Ultrasound effects on zinc recovery from EAF dust by sulfuric acid leaching. *Int. J. Miner. Met. Mater.* **2015**, *22*, 353–362. [CrossRef]
9. Ding, W.; Bao, S.; Zhang, Y.; Xiao, J. Efficient Selective Extraction of Scandium from Red Mud. *Miner. Process. Extr. Met. Rev.* **2023**, *44*, 304–312. [CrossRef]
10. Yin, X.; Opara, A.; Du, H.; Miller, J.D. Molecular dynamics simulations of metal–cyanide complexes: Fundamental considerations in gold hydrometallurgy. *Hydrometallurgy* **2010**, *106*, 64–70. [CrossRef]
11. Xie, Y.; Xie, S.; Chen, X.; Gui, W.; Yang, C.; Caccetta, L. An integrated predictive model with an on-line updating strategy for iron precipitation in zinc hydrometallurgy. *Hydrometallurgy* **2015**, *151*, 62–72. [CrossRef]
12. Park, J.; Jung, Y.; Kusumah, P.; Lee, J.; Kwon, K.; Lee, C. Application of Ionic Liquids in Hydrometallurgy. *Int. J. Mol. Sci.* **2014**, *15*, 15320–15343. [CrossRef]
13. Lai, Y.; Li, J.; Zhu, S.; Liu, K.; Xia, Q.; Huang, M.; Hu, G.; Zhang, H.; Qi, T. Recovery of rare earths, lithium, and fluorine from rare earth molten salt electrolytic slag by mineral phase reconstruction combined with vacuum distillation. *Sep. Purif. Technol.* **2023**, *310*, 123105. [CrossRef]
14. Yang, D.; Yu, M.; Mubula, Y.; Yuan, W.; Huang, Z.; Lin, B.; Mei, G.; Qiu, T. Recovering rare earths, lithium and fluorine from rare earth molten salt electrolytic slag using sub-molten salt method. *J. Rare Earths* **2023**, *42*, 1774–1781. [CrossRef]
15. Tong, Z.; Hu, X.; Wen, H. Effect of roasting activation of rare earth molten salt slag on extraction of rare earth, lithium and fluorine. *J. Rare Earths* **2023**, *41*, 300–308. [CrossRef]
16. Tian, L.; Chen, L.; Gong, A.; Wu, X.; Cao, C.; Xu, Z. Recovery of rare earths, lithium and fluorine from rare earth molten salt electrolytic slag via fluoride sulfate conversion and mineral phase reconstruction. *Miner. Eng.* **2021**, *170*, 106965. [CrossRef]
17. Wang, J.; Hu, H. Selective extraction of rare earths and lithium from rare earth fluoride molten-salt electrolytic slag by sulfation. *Miner. Eng.* **2021**, *160*, 106711. [CrossRef]
18. Mahfouz, M.G.; Galhoum, A.A.; Gomaa, N.A.; Abdel-Rehem, S.S.; Atia, A.A.; Vincent, T.; Guibal, E. Uranium extraction using magnetic nano-based particles of diethylenetriamine-functionalized chitosan: Equilibrium and kinetic studies. *Chem. Eng. J.* **2015**, *262*, 198–209. [CrossRef]
19. Larrabure, G.; Chero-Osorio, S.; Silva-Quiñones, D.; Benndorf, C.; Williams, M.; Gao, F.; Gamarra, C.; Alarcón, A.; Segura, C.; Teplyakov, A.; et al. Surface processes at a polymetallic (Mn-Fe-Pb) sulfide subject to cyanide leaching under sonication conditions and with an alkaline pretreatment: Understanding differences in silver extraction with X-ray photoelectron spectroscopy (XPS). *Hydrometallurgy* **2021**, *200*, 105544. [CrossRef]
20. Mubula, Y.; Yu, M.; Yang, D.; Niu, H.; Qiu, T.; Mei, G. Recovery of Rare Earths from Rare-Earth Melt Electrolysis Slag by Mineral Phase Reconstruction. *JOM* **2024**, *76*, 4732–4748. [CrossRef]
21. Cai, G.; Fung, K.; Ng, K.; Wibowo, C. Process development for the recycle of spent lithium ion batteries by chemical Precipitation. *Ind. Eng. Chem. Res.* **2014**, *53*, 18245–18259. [CrossRef]
22. Schipper, F.; Aurbach, D. A brief review: Past, present and future of lithium ion batteries. *Russ. J. Electrochem.* **2016**, *52*, 1095–1121. [CrossRef]
23. Luo, F.; Wei, C.; Zhang, C.; Gao, H.; Niu, J.; Ma, W.; Peng, Z.; Bai, Y.; Zhang, Z. Operando X-ray diffraction analysis of the degradation mechanisms of a spinel LiMn2O4 cathode in different voltage windows. *J. Energy Chem.* **2020**, *44*, 138–146. [CrossRef]

24. Chawla, N.; Bharti, N.; Singh, S. Recent Advances in Non-Flammable Electrolytes for Safer Lithium-Ion Batteries. *Batteries* **2019**, *5*, 19. [CrossRef]
25. Xia, S.; Huang, W.; Shen, X.; Liu, J.; Cheng, F.; Liu, J.-J.; Yang, X.; Guo, H. Rearrangement on surface structures by boride to enhanced cycle stability for LiNi0.80Co0.15Al0.05O2 cathode in lithium ion batteries. *J. Energy Chem.* **2020**, *45*, 110–118. [CrossRef]
26. Mubula, Y.; Yu, M.; Gu, H.; Wang, L.; Chen, M.; Qiu, T.; Mei, G. Recovery of rare earths from rare earth molten salt electrolytic slag using alkali phase reconstruction method with the aid of external electric field. *J. Rare Earths* **2024**, *43*, 2285–2294. [CrossRef]
27. Mubula, Y.; Yu, M.; Yang, D.; Niu, H.; Gu, H.; Qiu, T.; Mei, G. Microwave-assisted atmospheric alkaline leaching process and leaching kinetics of rare earth melt electrolysis slag. *Heliyon* **2024**, *10*, e32278. [CrossRef]
28. Kumari, A.; Dipali; Randhawa, N.S.; Sahu, S.K. Electrochemical treatment of spent NdFeB magnet in organic acid for recovery of rare earths and other metal values. *J. Clean. Prod.* **2021**, *309*, 127393. [CrossRef]
29. Çetintaş, S.; Bingöl, D. Performance evaluation of leaching processes with and without ultrasound effect combined with reagent-assisted mechanochemical process for nickel recovery from Laterite: Process optimization and kinetic evaluation. *Miner. Eng.* **2020**, *157*, 106562. [CrossRef]
30. Nalesso, S.; Bussemaker, M.J.; Sear, R.P.; Hodnett, M.; Lee, J. A review on possible mechanisms of sonocrystallisation in solution. *Ultrason. Sonochemistry* **2019**, *57*, 125–138. [CrossRef]
31. Ozonek, J. *Application of Hydrodynamic Cavitation in Environmental Engineering*; Reference and Research Book News; CRC Press: Boca Raton, FL, USA, 2012.
32. Chen, Y.; Truong, V.N.; Bu, X.; Xie, G. A review of effects and applications of ultrasound in mineral flotation. *Ultrason. Sonochemistry* **2020**, *60*, 104739. [CrossRef]
33. Altay, R.; Sadaghiani, A.K.; Sevgen, M.I.; Şişman, A.; Koşar, A. Numerical and Experimental Studies on the Effect of Surface Roughness and Ultrasonic Frequency on Bubble Dynamics in Acoustic Cavitation. *Energies* **2020**, *13*, 1126. [CrossRef]
34. Yasui, K. Unsolved Problems in Acoustic Cavitation. In *Handbook of Ultrasonics and Sonochemistry*; Springer: Berlin/Heidelberg, Germany, 2016; Volume 1.
35. Ezzatneshan, E.; Vaseghnia, H. Dynamics of an acoustically driven cavitation bubble cluster in the vicinity of a solid surface. *Phys. Fluids* **2021**, *33*, 123311. [CrossRef]
36. Nazari-Mahroo, H.; Pasandideh, K.; Navid, H.; Sadighi-Bonabi, R. Influence of liquid density variation on the bubble and gas dynamics of a single acoustic cavitation bubble. *Ultrasonics* **2020**, *102*, 106034. [CrossRef] [PubMed]
37. Chen, L.; He, J.; Zhu, L.; Yao, Q.; Sun, Y.; Guo, C.; Chen, H.; Yang, B. Efficient recovery of valuable metals from waste printed circuit boards via ultrasound-enhanced flotation. *Process. Saf. Environ. Prot.* **2022**, *169*, 869–878. [CrossRef]
38. Chen, X.; Li, S.; Wang, Y.; Jiang, Y.; Tan, X.; Han, W.; Wang, S. Recycling of LiFePO4 cathode materials from spent lithium-ion batteries through ultrasound-assisted Fenton reaction and lithium compensation. *Waste Manag.* **2021**, *136*, 67–75. [CrossRef]
39. Xin, C.; Xia, H.; Jiang, G.; Zhang, Q.; Zhang, L.; Xu, Y.; Cai, W. Mechanism and kinetics study on ultrasonic combined with oxygen enhanced leaching of zinc and germanium from germanium-containing slag dust. *Sep. Purif. Technol.* **2022**, *302*, 122167. [CrossRef]
40. Chen, B.; Bao, S.; Zhang, Y.; Li, S. A high-efficiency and sustainable leaching process of vanadium from shale in sulfuric acid systems enhanced by ultrasound. *Sep. Purif. Technol.* **2020**, *240*, 116624. [CrossRef]
41. Xue, J.; Lu, X.; DU, Y.; Mao, W.; Wang, Y.; Li, J. Ultrasonic-assisted Oxidation Leaching of Nickel Sulfide Concentrate. *Chin. J. Chem. Eng.* **2010**, *18*, 948–953. [CrossRef]
42. Li, H.; Li, S.; Peng, J.; Srinivasakannan, C.; Zhang, L.; Yin, S. Ultrasound augmented leaching of nickel sulfate in sulfuric acid and hydrogen peroxide media. *Ultrason. Sonochemistry* **2018**, *40*, 1021–1030. [CrossRef]
43. He, H.; Cao, J.; Duan, N. Synergistic effect between ultrasound and fierce mechanical activation towards mineral extraction: A case study of ZnO ore. *Ultrason. Sonochemistry* **2018**, *48*, 163–170. [CrossRef]
44. Mohammadnejad, S.; Provis, J.L.; van Deventer, J.S. Effects of grinding on the preg-robbing potential of quartz in an acidic chloride medium. *Miner. Eng.* **2013**, *52*, 31–37. [CrossRef]
45. Kaupp, G. Mechanochemistry: The varied applications of mechanical bond-breaking. *CrystEngComm* **2009**, *11*, 388–403. [CrossRef]
46. Wang, J.; Faraji, F.; Ghahreman, A. Effect of Ultrasound on the Oxidative Copper Leaching from Chalcopyrite in Acidic Ferric Sulfate Media. *Minerals* **2020**, *10*, 633. [CrossRef]
47. Li, S.; Chen, W.; Yin, S.; Ma, A.; Yang, K.; Xie, F.; Zhang, L.; Peng, J. Impacts of ultrasound on leaching recovery of zinc from low grade zinc oxide ore. *Green Process Synth.* **2015**, *4*, 323–328. [CrossRef]
48. Zhang, L.; Li, H.; Peng, J.; Srinivasakannan, C.; Li, S.; Yin, S. Microwave and ultrasound augmented leaching of complicated zinc oxide ores in ammonia and ammonium citrate solutions. *Metals* **2017**, *7*, 216. [CrossRef]
49. Knaislová, A.; Vu, H.N.; Dvořák, P. Microwave and Ultrasound Effect on Ammoniacal Leaching of Deep-Sea Nodules. *Minerals* **2018**, *8*, 351. [CrossRef]
50. Li, X.; Li, T.; Gao, J.; Huang, H.; Li, L.; Li, J. A novel "green" solvent to deeply purify quartz sand with high yields: A case study. *J. Ind. Eng. Chem.* **2016**, *35*, 383–387. [CrossRef]

51. Zhang, Z.; Li, J.; Li, X.; Huang, H.; Zhou, L.; Xiong, T. High efficiency iron removal from quartz sand using phosphoric acid. *Int. J. Miner. Process* **2012**, *114–117*, 30–34. [CrossRef]
52. Du, F.; Li, J.; Li, X.; Zhang, Z. Improvement of iron removal from silica sand using ultrasound-assisted oxalic acid. *Ultrason. Sonochemistry* **2011**, *18*, 389–393. [CrossRef]
53. Chen, B.; Bao, S.; Zhang, Y. Synergetic strengthening mechanism of ultrasound combined with calcium fluoride towards vanadium extraction from low-grade vanadium-bearing shale. *Int. J. Min. Sci. Technol.* **2021**, *31*, 1095–1106. [CrossRef]
54. Yang, J.-H.; He, L.-H.; Liu, X.-H.; Ding, W.-T.; Song, Y.-F.; Zhao, Z.-W. Comparative kinetic analysis of conventional and ultrasound-assisted leaching of scheelite by sodium carbonate. *Trans. Nonferrous Met. Soc. China* **2018**, *28*, 775–782. [CrossRef]
55. Johansson, Ö.; Pamidi, T.; Shankar, V. Extraction of tungsten from scheelite using hydrodynamic and acoustic cavitation. *Ultrason. Sonochemistry* **2021**, *71*, 105408. [CrossRef] [PubMed]
56. Fu, L.; Zhang, L.; Wang, S.; Cui, W.; Peng, J. Synergistic extraction of gold from the refractory gold ore via ultrasound and chlorination-oxidation. *Ultrason. Sonochemistry* **2017**, *37*, 471–477. [CrossRef] [PubMed]
57. Gui, Q.; Hu, Y.; Wang, S.; Zhang, L. Mechanism of synergistic pretreatment with ultrasound and ozone to improve gold and silver leaching percentage. *Appl. Surf. Sci.* **2022**, *576*, 151726. [CrossRef]
58. Cilek, E.C.; Ciftci, H.; Karagoz, S.G.; Tuzci, G. Extraction of silver from a refractory silver ore by sono-cyanidation. *Ultrason. Sonochemistry* **2020**, *63*, 104965. [CrossRef]
59. Zhao, Z.; Ding, W.; Liu, X.; Liang, Y. Effect of ultrasound on kinetics of scheelite leaching in sodium hydroxide. *Can. Met. Quart.* **2013**, *52*, 138–145. [CrossRef]
60. Zhu, P.; Zhang, X.-J.; Li, K.-F.; Qian, G.-R.; Zhou, M. Kinetics of leaching refractory gold ores by ultrasonic-assisted electro-chlorination. *Int. J. Miner. Met. Mater.* **2012**, *19*, 473–477. [CrossRef]
61. Yin, S.; Pei, J.; Jiang, F.; Li, S.; Peng, J.; Zhang, L.; Ju, S.; Srinivasakannan, C. Ultrasound-assisted leaching of rare earths from the weathered crust elution-deposited ore using magnesium sulfate without ammonia-nitrogen pollution. *Ultrason. Sonochemistry* **2018**, *41*, 156–162. [CrossRef]
62. Chanturiya, V.; Minenko, V.; Samusev, A.; Chanturia, E.; Koporulina, E.; Bunin, I.; Ryazantseva, M. The Effect of Energy Impacts on the Acid Leaching of Eudialyte Concentrate. *Miner. Process. Extr. Met. Rev.* **2021**, *42*, 484–495. [CrossRef]
63. Mubula, Y.; Yu, M.; Yang, D.; Lin, B.; Guo, Y.; Qiu, T. Recovery of valuable elements from solid waste with the aid of external electric field: A review. *J. Environ. Chem. Eng.* **2023**, *11*, 111237. [CrossRef]
64. Esmaeili, M.; Rastegar, S.; Beigzadeh, R.; Gu, T. Ultrasound-assisted leaching of spent lithium ion batteries by natural organic acids and H_2O_2. *Chemosphere* **2020**, *254*, 126670. [CrossRef]
65. Xiao, X.; Hoogendoorn, B.W.; Ma, Y.; Sahadevan, S.A.; Gardner, J.M.; Forsberg, K.; Olsson, R.T. Ultrasound-assisted extraction of metals from Lithium-ion batteries using natural organic acids. *Green Chem.* **2021**, *23*, 8519–8532. [CrossRef]
66. Ding, W.; Bao, S.; Zhang, Y.; Xiao, J. Mechanism and kinetics study on ultrasound assisted leaching of gallium and zinc from corundum flue dust. *Miner. Eng.* **2022**, *183*, 107624. [CrossRef]
67. Hosseinzadeh, F.; Rastegar, S.O.; Ashengroph, M.; Gu, T. Ultrasound-assisted Fenton-like reagent to leach precious metals from spent automotive catalysts: Process optimization and kinetic modeling. *Int. J. Environ. Sci. Technol.* **2021**, *18*, 3449–3458. [CrossRef]
68. Zhu, R.; Wang, S.; Chen, Y.; Xiang, D.; Zhang, L.; Liu, J.; Ye, J. Ultrasound enhanced in-situ chemical oxidation for leaching Ag from zinc leaching residue and response surface optimization. *Chem. Eng. J.* **2024**, *489*, 151243. [CrossRef]
69. Kong, J.; Xing, P.; Wei, D.; Jin, X.; Zhuang, Y. Ultrasound-Assisted Leaching of Iron from Silicon Diamond-Wire Saw Cutting Waste. *JOM* **2021**, *73*, 791–800. [CrossRef]
70. Xie, H.; Li, S.; Guo, Z.; Xu, Z. Extraction of lead from electrolytic manganese anode mud by microwave coupled ultrasound technology. *J. Hazard. Mater.* **2021**, *407*, 124622. [CrossRef]
71. Oza, R.; Shah, N.; Patel, S. Recovery of nickel from spent catalysts using ultrasonication-assisted leaching. *J. Chem. Technol. Biotechnol.* **2011**, *86*, 1276–1281. [CrossRef]
72. Wang, X.; Yang, D.-J.; Srinivasakannan, C.; Peng, J.-H.; Duan, X.-H.; Ju, S.-H. A Comparison of the Conventional and Ultrasound-Augmented Leaching of Zinc Residue Using Sulphuric Acid. *Arab. J. Sci. Eng.* **2014**, *39*, 163–173. [CrossRef]
73. Liu, J.; Wang, S.; Zhang, Y.; Zhang, L.; Kong, D. Synergistic mechanism and decopperization kinetics for copper anode slime via an integrated ultrasound-sodium persulfate process. *Appl. Surf. Sci.* **2022**, *589*, 153032. [CrossRef]
74. Huang, Z.; Xie, F.; Ma, Y. Ultrasonic recovery of copper and iron through the simultaneous utilization of Printed Circuit Boards (PCB) spent acid etching solution and PCB waste sludge. *J. Hazard. Mater.* **2011**, *185*, 155–161. [CrossRef]
75. Wang, S.; Cui, W.; Zhang, G.; Zhang, L.; Peng, J. Ultra fast ultrasound-assisted decopperization from copper anode slime. *Ultrason. Sonochemistry* **2017**, *36*, 20–26. [CrossRef]
76. Turan, M.D.; Sari, Z.A.; Demiraslan, A. Ultrasound-assisted leaching and kinetic study of blended copper slag. *Met. Mater. Trans. B* **2019**, *50*, 1949–1956. [CrossRef]
77. Nguyen, T.T.N.; Lee, M.S. Improvement of Alumina Dissolution from the Mechanically Activated Dross Using Ultrasound-Assisted Leaching. *Korean J. Met. Mater.* **2019**, *57*, 154–161. [CrossRef]

78. Li, X.; Xing, P.; Du, X.; Gao, S.; Chen, C. Influencing factors and kinetics analysis on the leaching of iron from boron carbide waste-scrap with ultrasound-assisted method. *Ultrason. Sonochemistry* **2017**, *38*, 84–91. [CrossRef]
79. Masoum, H.G.; Rastegar, S.O.; Khamforoush, M. Ultrasound-Assisted Leaching of Vanadium and Yttrium from Coal Ash: Optimization, Kinetic and Thermodynamic Study. *Chem. Eng. Technol.* **2021**, *44*, 2249–2256. [CrossRef]
80. Vyas, S.; Ting, Y.-P. Effect of ultrasound on bioleaching of hydrodesulphurization spent catalyst. *Environ. Technol. Innov.* **2019**, *14*, 100310. [CrossRef]
81. Sadeghi, S.M.; Jesus, J.; Pinto, E.; Almeida, A.A.; Soares, H.M. A simple, efficient and selective process for recycling La (and Al) from fluid cracking catalysts using an environmentally friendly strategy. *Miner. Eng.* **2020**, *156*, 106375. [CrossRef]
82. Behera, S.; Panda, S.K.; Mandal, D.; Parhi, P. Ultrasound and Microwave assisted leaching of neodymium from waste magnet using organic solvent. *Hydrometallurgy* **2019**, *185*, 61–70. [CrossRef]
83. Jiang, F.; Chen, Y.; Ju, S.; Zhu, Q.; Zhang, L.; Peng, J.; Wang, X.; Miller, J.D. Ultrasound-assisted leaching of cobalt and lithium from spent lithium-ion batteries. *Ultrason. Sonochemistry* **2018**, *48*, 88–95. [CrossRef]
84. Ning, P.; Meng, Q.; Dong, P.; Duan, J.; Xu, M.; Lin, Y.; Zhang, Y. Recycling of cathode material from spent lithium ion batteries using an ultrasound-assisted DL-malic acid leaching system. *Waste Manag.* **2020**, *103*, 52–60. [CrossRef] [PubMed]
85. Wen, J.; Jiang, T.; Gao, H.; Liu, Y.; Zheng, X.; Xue, X. Comparison of Ultrasound-Assisted and Regular Leaching of Vanadium and Chromium from Roasted High Chromium Vanadium Slag. *JOM* **2018**, *70*, 155–160. [CrossRef]
86. Marafi, M.; Stanislaus, A. Waste Catalyst Utilization: Extraction of Valuable Metals from Spent Hydroprocessing Catalysts by Ultrasonic-Assisted Leaching with Acids. *Ind. Eng. Chem. Res.* **2011**, *50*, 9495–9501. [CrossRef]
87. Pinto, I.S.; Soares, H.M. Selective leaching of molybdenum from spent hydrodesulphurisation catalysts using ultrasound and microwave methods. *Hydrometallurgy* **2012**, *129–130*, 19–25. [CrossRef]
88. Wang, L.; Chao, L.; Qu, W.; Xu, S.; Zhang, L.; Peng, J.; Ye, X. Ultrasound-assisted oil removal of γ-Al_2O_3-based spent hydrodesulfurization catalyst and microwave roasting recovery of metal Mo. *Ultrason. Sonochemistry* **2018**, *49*, 24–32. [CrossRef]
89. Toache-Pérez, A.D.; Bolarín-Miró, A.M.; Jesús, F.S.-D.; Lapidus, G.T. Facile method for the selective recovery of Gd and Pr from LCD screen wastes using ultrasound-assisted leaching. *Sustain. Environ. Res.* **2020**, *30*, 20. [CrossRef]
90. Tunsu, C.; Ekberg, C.; Retegan, T. Characterization and leaching of real fluorescent lamp waste for the recovery of rare earth metals and mercury. *Hydrometallurgy* **2014**, *144–145*, 91–98. [CrossRef]
91. Zhang, L.; Song, Q.; Xu, X.; Xu, Z. Process simulation of Ohno continuous casting for single crystal copper prepared from scrap copper in waste printed circuit boards. *Waste Manag.* **2021**, *124*, 94–101. [CrossRef]
92. Li, J.; Jiang, Y.; Xu, Z. Eddy current separation technology for recycling printed circuit boards from crushed cell phones. *J. Clean. Prod.* **2017**, *141*, 1316–1323. [CrossRef]
93. Niu, B.; E, S.; Song, Q.; Xu, Z.; Han, B.; Qin, Y. Physicochemical reactions in e-waste recycling. *Nat. Rev. Chem.* **2024**, *8*, 569–586. [CrossRef]